J|A|C|S
ARTICLES
Published on Web 05/04/2002

Locked Nucleic Acid (LNA) Recognition of RNA: NMR Solution Structures of LNA:RNA Hybrids

Michael Petersen,* Kent Bondensgaard,† Jesper Wengel, and Jens Peter Jacobsen

Contribution from the Nucleic Acid Center, §Department of Chemistry, University of Southern Denmark, Odense University, DK-5230 Odense M, Denmark

Received October 3, 2001

Abstract: Locked nucleic acids (LNAs) containing one or more 2′-*O*,4′-*C*-methylene-linked bicyclic ribonucleoside monomers possess a number of the prerequisites of an effective antisense oligonucleotide, e.g. unprecedented helical thermostability when hybridized with cognate RNA and DNA. To acquire a detailed understanding of the structural features of LNA giving rise to its remarkable properties, we have conducted structural studies by use of NMR spectroscopy and now report high-resolution structures of two LNA:RNA hybrids, the LNA strands being d(5′-CTGA**T**^{L}ATGC-3′) and d(5′-C**T**^{L}GA**T**^{L}A**T**^{L}GC-3′), respectively, **T**^{L} denoting a modified LNA monomer with a thymine base, along with the unmodified DNA:RNA hybrid. In the structures, the LNA nucleotides are positioned as to partake in base stacking and Watson−Crick base pairing, and with the inclusion of LNA nucleotides, we observe a progressive change in duplex geometry toward an A-like duplex structure. As such, with the inclusion of three LNA nucleotides, the hybrid adopts an almost canonical A-type duplex geometry, and thus it appears that the number of modifications has reached a saturation level with respect to structural changes, and that further incorporations would furnish only minute changes in the duplex structure. We attempt to rationalize the conformational steering induced by the LNA nucleotides by suggesting that the change in electronic density at the brim of the minor groove, introduced by the LNA modification, is causing an alteration of the pseudorotational profile of the 3′-flanking nucleotide, thus shifting this sugar equilibrium toward *N*-type conformation.

Introduction

In recent years, the acknowledgment of the antisense strategy for the treatment of malfunctional genes has prompted the synthesis of a plethora of chemically modified nucleic acids.[1−3] The *modus operandi* of the antisense approach is the arresting of a specific mRNA by its cognate antisense oligonucleotide (AO), thus inactivating the expression of the unwanted protein coded for by that given mRNA. This approach, in principle, allows switching off protein expression at will.

There are several mechanisms by which AOs may terminate the activity of the target mRNA, e.g. inhibition of splicing, translation arrest, and degradation of the mRNA by RNase H. The most studied, and possibly the mechanism resulting in the most potent AOs, is RNase H activation. Ideally, RNase H selectively cleaves the RNA strand of AO:RNA hybrids, thus inactivating the mRNA and rendering the AO free to interact with yet another cognate mRNA. High affinity and selectivity toward the cognate RNA by the AO are important, as otherwise, the binding would occur infrequently, thus lowering the efficacy of the drug, and possibly introduce unwanted toxicity due to nonselective binding of nontargeted mRNAs. In addition, the target mRNA may not be readily accessible as mRNAs are known to form secondary structures, e.g. hairpin loops.

In the quest for the perfect antisense molecule, an immense number of chemically modified nucleotides have been synthesized and their binding affinity toward cognate RNAs evaluated. Generally, it appears that nucleotides favoring an *N*-type sugar conformation, e.g. 2′-*O*-alkyl modified riboses[4] or phosphoramidates,[5] are displaying an increased helical thermostability, relative to native DNA, when hybridized with complementary RNAs.[6] Although structures have been determined of nucleic acids incorporating *N*-type favoring nucleotides, little is known about the features underlying the increase in thermostability facilitated by these nucleotides. Thus, at present, no structure-activity relationship exists paving the way for rational design of modified nucleic acids.

Recently one such *N*-type favoring nucleotide analogue, LNA (Chart 1), has been introduced.[7−10] LNA (the term "LNA" is

* To whom correspondence should be addressed. E-mail: mip@chem.sdu.dk.

† Present address: Health Care Chemistry, Novo Nordisk A/S, Novo Nordisk Park, DK-2760 Måløv, Denmark.

§ A research centre funded by the Danish National Research Foundation for studies on the chemical biology of nucleic acids.

(1) Hélène, C.; Toulmé, J.-J. *Biochim. Biophys. Acta* **1990**, *1049*, 99.
(2) Flanagan, W. M. *Cancer Metast. Rev.* **1998**, *17*, 169.
(3) Uhlmann, E.; Peyman, A. *Chem. Rev.* **1990**, *90*, 543.
(4) Manoharan, M. *Biochim. Biophys. Acta* **1999**, *1489*, 117.
(5) Gryaznov, S. M. *Biochim. Biophys. Acta* **1999**, *1489*, 131.
(6) Freier, S. M.; Altmann, K.-H. *Nucleic Acids Res.* **1997**, *25*, 4429.
(7) Koshkin, A. A.; Singh, S. K.; Nielsen, P.; Rajwanshi, V. K.; Kumar, R.; Meldgaard, M.; Olsen, C. E.; Wengel, J. *Tetrahedron* **1998**, *54*, 3607.
(8) Koshkin, A. A.; Rajwanshi, V. K.; Wengel, J. *Tetrahedron Lett.* **1998**, *39*, 4381.
(9) Singh, S. K.; Nielsen, P.; Koshkin, A. A.; Wengel, J. *Chem. Commun.* **1998**, 455.

10.1021/ja012288d CCC: $22.00

Chart 1. The LNA Nucleotide and Sugar Puckering Conformations of Nucleotides

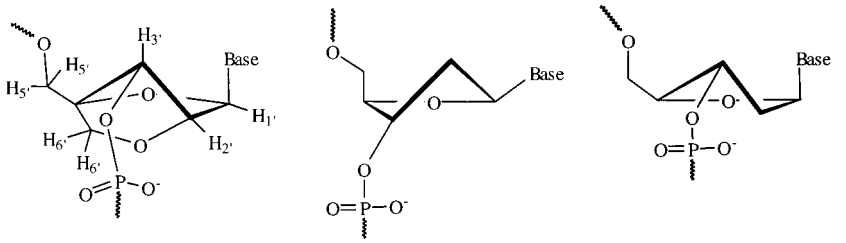

LNA **C2'-*endo* (*S*-type)** **C3'-*endo* (*N*-type)**

Chart 2. The Numbering Schemes of the Oligonucleotides Studied

		1	2	3	4	5	6	7	8	9	
DNA:RNA	**5'-d(**	**C**	**T**	**G**	**A**	**T**	**A**	**T**	**G**	**C**	**)-3'**
	3'-r(	**G**	**A**	**C**	**U**	**A**	**U**	**A**	**C**	**G**	**)-5'**
		18	*17*	*16*	*15*	*14*	*13*	*12*	*11*	*10*	
LNA1:RNA	**5'-d(**	**C**	**T**	**G**	**A**	***T*^{L}**	**A**	**T**	**G**	**C**	**)-3'**
	3'-r(	**G**	**A**	**C**	**U**	**A**	**U**	**A**	**C**	**G**	**)-5'**
LNA3:RNA	**5'-d(**	**C**	***T*^{L}**	**G**	**A**	***T*^{L}**	**A**	***T*^{L}**	**G**	**C**	**)-3'**
	3'-r(	**G**	**A**	**C**	**U**	**A**	**U**	**A**	**C**	**G**	**)-5'**

***T*^{L}** *denotes an LNA thymine nucleotide.*

henceforth used to denote an oligonucleotide containing one or more 2′-*O*,4′-*C*-methylene-linked bicyclic ribonucleoside monomers; LNA nucleotides) possesses a number of the prerequisites of an attractive AO, e.g. stability toward 3′-exonucleolytic degradation[9,11] and effective delivery into living MCF-7 breast cancer cells by Lipofectin mediated transfection.[11] In addition, LNA possesses a favorable toxicity profile when administered in vivo.[11] Both fully modified LNA, composed entirely of LNA nucleotide monomers, as well as mix-mer LNA, composed of a mixture of LNA and DNA nucleotide monomers, display unprecedented binding affinity toward complementary RNA or DNA combined with conserved or even improved sequence specificity.[7,9,10,12−15] LNA shows no significant sequence dependence in the increased binding affinities and therefore provides an excellent tool for targeting any RNA or DNA sequence for use both as an AO and in diagnostic applications.

To understand and delineate the properties of LNA, we have carried out a systematic study of nucleic acid hybrids containing LNA nucleotides. Previously, we have published sugar conformations and interproton distances derived from NMR experiments together with CD spectra of two nonamer LNA:RNA hybrids, containing one and three modifications, respectively, and the corresponding unmodified DNA:RNA reference hybrid (the hybrids studied are shown in Chart 2).[16] In accordance with earlier studies,[17−19] our results showed that the reference DNA:RNA hybrid assumes a conformation between A- and B-type duplex geometry, with the RNA strand having an overall A-type structure and the DNA strand a structure intermediate of A- and B-type. Upon incorporation of LNA modifications in the DNA strand, the structure of this strand changes toward A-type. However, the effect is entirely local, only nucleotides flanking a modification are affected (most pronounced for the nucleotides following in the 3′-direction). When three modifications are introduced, both sugar conformations and interproton distances of the deoxyribose nucleotides are those peculiar of an overall A-type structure.

To acquire a more detailed understanding of the structural features of LNA underlying its remarkable properties, we have proceeded with our structural studies and now report high-resolution structures of the two LNA:RNA hybrids along with the DNA:RNA reference hybrid (Chart 2). The hybrid structures have been determined by employing NOE derived distance restraints in Simulated Annealing schemes rendering average NOE structures.

Methods and Materials

Sample Preparation. The modified oligonucleotides were synthesized as described elsewhere[7,9] and were purified by site-exclusion on a Sephadex G15 column. The samples were obtained by dissolving equimolar amounts of the two single strands in 0.5 mL of 10 mM sodium phosphate buffer (pH 7.0), 100 mM NaCl, and 0.05 mM NaEDTA. For experiments carried out in D_2O, the duplex solutions were lyophilized three times from D_2O and redissolved in 99.96% D_2O (Cambridge Isotope Laboratories). Mixtures of 90% H_2O and 10% D_2O (0.5 mL) were used for experiments examining exchangeable protons. The final concentrations of the hybrids were 0.7−2.0 mM.

NMR Experiments. NMR experiments were performed on either a Varian UNITY 500 spectrometer or a Varian INOVA 750 spectrometer at 25 °C. NOESY spectra (mixing times: 60, 120, and 200 ms at 750 MHz for LNA3:RNA; 100, 200, and 300 ms at 500 MHz for LNA1:RNA; 60, 120, 200, and 300 ms at 750 MHz for DNA:RNA) were acquired in D_2O using 512 t_1-experiments with 64 scans, 2048 complex points in t_2, a pulse repetition time of 3.7 s, and spectral widths of 7500 Hz at 750 MHz and 5000 Hz at 500 MHz, respectively. The States phase cycling scheme was used and the residual signal from HOD was removed by low-power presaturation. Inversion recovery experiments to extract the T_1 relaxation rates were also obtained. NOESY spectra in H_2O with 200 ms mixing times were acquired using the WATERGATE NOESY pulse sequence using 4096 complex points in t_2 and 512 t_1-experiments with a spectral width of 15000 Hz at 750 MHz.

(10) Obika, S.; Nanbu, D.; Hari, Y.; Andoh, J.; Morio, K.; Doi, T.; Imanishi, T. *Tetrahedron Lett.* **1998**, *39*, 5401.
(11) Wahlestedt, C.; Salmi, P.; Good, L.; Kela, J.; Johnsen, T.; Hökfelt, T.; Broberger, C.; Porreca, F.; Koshkin, A.; Jacobsen, M. H.; Wengel, J. *Proc. Natl. Acad. Sci. U.S.A.* **2000**, *97*, 5633.
(12) Koshkin, A. A.; Nielsen, P.; Meldgaard, M.; Rajwanshi, V. K.; Singh, S. K.; Wengel, J. *J. Am. Chem. Soc.* **1998**, *120*, 13252.
(13) Singh, S. K.; Wengel, J. *Chem. Commun.* **1998**, 1247.
(14) Singh, S. K.; Kumar, R.; Wengel, J. *J. Org. Chem.* **1998**, *63*, 3, 10035.
(15) Wengel, J. *Acc. Chem. Res.* **1998**, *32*, 301.
(16) Bondensgaard, K.; Petersen, M.; Singh, S. K.; Rajwanshi, V. K.; Wengel, J.; Jacobsen, J. P. *Chem. Eur. J.* **2000**, *6*, 2687.
(17) Nielsen, K. E.; Singh, S. K.; Wengel, J.; Jacobsen, J. P. *Bioconj. Chem.* **2000**, *11*, 228.
(18) Nielsen, C. B.; Singh, S. K.; Wengel, J.; Jacobsen, J. P. *J. Biomol. Struct. Dyn.* **1999**, *17*, 175.
(19) Petersen, M.; Nielsen, C. B.; Nielsen, K. E.; Jensen, G. A.; Bondensgaard, K.; Singh, S. K.; Rajwanshi, V. K.; Koshkin, A. A.; Dahl, B. M.; Wengel, J.; Jacobsen, J. P. *J. Mol. Recognit.* **2000**, *13*, 44.

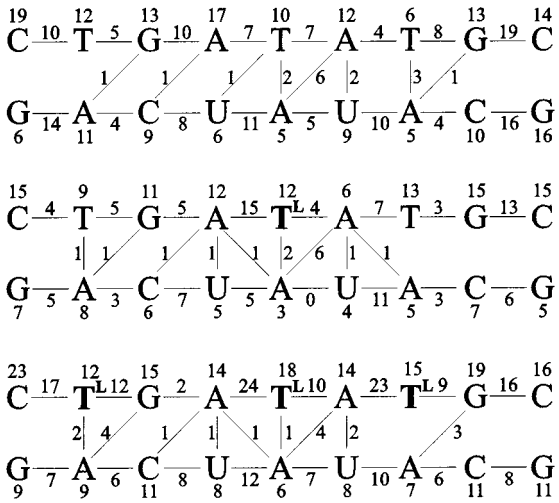

Figure 1. The distribution of the NOE restraints obtained from RANDMARDI calculations: DNA:RNA (top), LNA1:RNA (middle), and LNA3:RNA (bottom). The numbers of intranucleotide, sequential, and cross-strand restraints are indicated. In addition to the restraints shown, two further restraints, between T7 and C9 (DNA:RNA) and T^L5 and T^L7 (LNA3:RNA), were obtained.

TOCSY spectra with mixing times of 30, 60, and 90 ms were obtained in the TPPI mode at 500 MHz. Gradient $^1H-^{13}C$ HSQC spectra were obtained at 500 MHz. *J*-scaled $^1H-^{31}P$ HMBC spectra[20] were obtained at 500 MHz with the scaling parameter $\kappa = 5$ using 56 t_1-experiments and 4096 complex points in t_2 with a spectral width of 600 Hz in the ^{31}P domain. A gradient selection of both *N*- and *P*-type spectra was used.

The acquired data were processed at optimal conditions using FELIX (version 97.2, MSI, San Diego, CA). Particularly, the NOESY spectra recorded in the build-ups of DNA:RNA and LNA3:RNA and the NOESY spectra recorded in H_2O were linear predicted from 256 points to 512 points in t_1, and the *J*-scaled $^1H-^{31}P$ HMBC spectra were linear predicted from 28 points to 56 points in t_1.

Distance Restraints. The extraction of distance restraints from the NOE build-ups was described in a previous paper.[16] Totals of 354 (DNA:RNA), 270 (LNA1:RNA), and 423 (LNA3:RNA) distance restraints were obtained from 2D NOE cross-peak intensities using a full relaxation matrix analysis with the program RANDMARDI;[21] the distributions of NOE restraints in the three hybrids are shown in Figure 1. Final distance bounds were determined by averaging upper and lower bounds in all MARDIGRAS[22] calculations performed in the RANDMARDI procedure; a further 0.2 (LNA3:RNA) or 0.3 Å (DNA:RNA and LNA1:RNA) was added to the upper distance bounds returned by MARDIGRAS. The average flat well widths thus obtained were 1.07 (DNA:RNA), 0.66 (LNA1:RNA), and 1.01 Å (LNA3:RNA), respectively. A further 58 restraints with loose bounds were derived from the NOESY spectrum in H_2O of the LNA3:RNA hybrid. These distance restraints were derived using the "Isolated Spin-Pair Approximation" (ISPA) with cytosine H5−H6 cross-peaks as reference peaks. Due to the inherent error in ISPA, and the possibility of exchange of labile protons, wide bounds (ISPA distance ± 1 Å) were set for these restraints.

In addition to the experimental restraints above, Watson−Crick hydrogen bond restraints (22 per hybrid) were included in the calculations. Target values for these restraints were taken from crystallographic data.[23]

All distance restraints were incorporated into the AMBER potential energy by a flat-well pseudo potential with the form:

$$\begin{aligned} E_{NOE} &= -K_{NOE}r + (r_1 - 0.25\ \text{Å})K_{NOE}, \text{ if } r \le r_1 - 0.5\ \text{Å} \\ &= K_{NOE}(r - r_1)^2, \text{ if } r_1 - 0.5\text{Å} < r < r_1 \\ &= 0, \text{ if } r_1 \le r \le r_2 \\ &= K_{NOE}(r - r_2)^2, \text{ if } r_2 < r < r_2 + 0.5\ \text{Å} \\ &= K_{NOE}r + (r_2 + 0.25\ \text{Å})K_{NOE}, \text{ if } r \ge r_2 + 0.5\ \text{Å} \end{aligned}$$

where the force constants, K_{NOE}, are in units of kcal/(mol Å) or kcal/(mol Å^2) and r_1 and r_2 are the lower and upper distance bounds, respectively.

$^3J_{HH}$ Coupling Constants. Deoxyribose proton coupling constants were obtained by simulating DQF-COSY spectra as previously described.[16,19] The proton coupling constants were not included in any calculation but rather employed to validate the structures generated. For calculation of theoretical deoxyribose proton coupling constants, the Karplus relation and parametrization of Altona and co-workers was used.[24,25] Comparison between theoretically calculated and experimentally derived coupling constants was carried out using the J_{RMSD} indicator:

$$J_{RMSD} = \sqrt{\frac{1}{N}\sum (J_{calc} - J_{exp})^2}$$

Simulated Annealing. All calculations were performed with the AMBER6[26] suite of programs on SGI/O2 workstations. A simulated annealing (SA) protocol was utilized to obtain the average structures of the three hybrids. Two different starting structures (A- and B-form duplexes), obtained with the *nucgen* module of AMBER6, were used. The appropriate nucleotides were modified to LNA nucleotides and atomic charges for the modified nucleotides were calculated using the RESP procedure (a table showing the atomic charges for LNA thymidine is included in Supporting Information).[27]

Each structure was initially restrained energy minimized before being subjected to 28 ps of molecular dynamics in time steps of 1 fs: 4 ps at 600 K followed by cooling to 300 K over 24 ps. Finally, a further restrained energy minimization was carried out. In the SA schemes force constants of $K_{NOE} = 50$ kcal/(mol Å^2) were used. A distance-dependent dielectric constant, $\epsilon = 4r$, was used and the nonbonded cutoff was 30 Å.

For the LNA1:RNA hybrid, backbone angle restraints were included in the SA procedure. The α, β, and γ angles were restrained in the two terminal nucleotides in each strand with the flat-well potential as follows: α, −90° to −30°; β, 170−230°; and γ, 20−90°. These angular restraints are suitable to accommodate both A- and B-form duplex geometries. A total of 23 such angular restraints were included in the refinement with force constants $K_{angle} = 15$ kcal/(mol rad^2). Moreover, in the LNA1:RNA hybrid, the ϵ backbone angles were constrained by $^3J_{HP}$ coupling constants gauged from a *J*-scaled ^1H, ^{31}P-HMBC spectrum.[20] The coupling constants were incorporated directly into the refinement procedure with a flat-well potential similar to that of the distance restraints and the Karplus equation of $^3J_{HP} = 15.3\cos^2\theta - 6.1\cos\theta + 1.6$, where θ is the H3′−C3′−O3′−P torsion angle and ϵ

(20) Gotfredsen, C. H.; Meissner, A.; Duus, J. Ø.; Sørensen, O. W. *Magn. Reson. Chem.* **2000**, *38*, 692.
(21) Liu, H.; Spielmann, H. P.; Ulyanov, N. A.; Wemmer, D. E.; James, T. L. *J. Biomol. NMR* **1995**, *6*, 390.
(22) Borgias, B. A.; Gochin, M.; Kerwood, D.; James, T. L. *Prog. Nucl. Magn. Reson. Spectrosc.* **1990**, *22*, 83.
(23) Saenger, W. *Principles of Nucleic Acid Structure*; Springer-Verlag: New York, 1984.
(24) de Leeuw, F. A. A. M.; Altona, C. *J. Comput. Chem.* **1983**, *4*, 428.
(25) Donders, L. A.; de Leeuw, F. A. A. M.; Altona, C. *Magn. Reson. Chem.* **1989**, *27*, 556.
(26) Case, D. A.; Pearlman, D. A.; Caldwell, J. W.; Cheatham, T. E. III; Ross, W. S.; Simmerling, C. L.; Darden, T. A.; Merz, K. M.; Stanton, R. V.; Cheng, A. L.; Vincent, J. J.; Crowley, M.; Tsui, V.; Radmer, R. J.; Duan, Y.; Pitera, J.; Massura, I.; Seibel, G. L.; Singh, U. C.; Weiner, P.; Kollman, P. A. *AMBER 6*; University of California, San Francisco, 2000.
(27) Bayly, C. I.; Cieplak, P.; Cornell, W. D.; Kollman, P. A. *J. Phys. Chem.* **1993**, *97*, 10269.

Table 1. Structural Parameters for the Average NOE Structures[a]

	structure	E_{AMBER} (kcal/mol)	E_{NOE} (kcal/mol)	Δd_{av} (Å)	Δd_{av} (Hz)	RMSD vs NMR (Å)
DNA:RNA	A-type	−52.5	3729.4	0.313	4.9	1.74(0.09)
	B-type	−38.9	7333.0	0.519	2.6	3.30(0.19)
	NMR	200.6(4.1)	124.2(1.5)	0.043	2.0	0.54(0.19)[b]
LNA1:RNA	A-type	−35.7	3174.4	0.295	5.2	1.73(0.12)
	B-type	−17.7	4227.9	0.387	2.5	2.98(0.12)
	NMR	66.2(1.6)	10.2(0.1)	0.035	2.5	0.26(0.08)[b]
LNA3:RNA	A-type	−5.3	1492.4	0.124	*c*	0.83(0.05)
	B-type	8.3	8341.4	0.450	*c*	3.91(0.14)
	NMR	127.8(3.1)	80.2(1.6)	0.025	*c*	0.47(0.32)[b]

[a] Force field (E_{AMBER}) and restraint (E_{NOE}) energies, average restraint violations (Δd_{av}), coupling constant RMSDs (J_{RMSD}), and pairwise atomic RMSDs for the starting structures and average NMR structures for the various hybrids. All-atomic RMSDs were calculated for all atoms of the seven internal base pairs. Where applicable, standard deviations are included in brackets. [b] Atomic RMSDs for the 20 structures calculated from A-form starting geometry. [c] No J_{RMSD} values calculated as only coupling constants in terminal sugars were determined.

$= \theta - 120°$.[28] The flat-well was 0−4.5 Hz for deoxyribonucleotides and 0−8.0 Hz for ribonucleotides (including LNAs). A total of 16 coupling constant restraints were included with force constants $K_J =$ 25 kcal/(mol Hz^2).

Results

The Average Structures. A total of 40 structures were calculated for each of the hybrids employing the SA-protocol described above. Twenty random sets of initial velocities for each of the two starting structures were used. RMSD values for the structures generated are included in Table 1. Generally, we obtained good convergence within the families of structures generated from both A- and B-form starting geometries. However, for the LNA3:RNA hybrid, six of the calculated structures from the B-form starting geometry displayed high restraint and force field energies, and by inspection of the structures generated, these structures turned out to be outliers. If these six outliers are disregarded, the RMSD for the remaining 34 structures was 0.58 Å for the seven internal base pairs for this hybrid. For the other hybrids, the corresponding RMSDs were 0.79 (DNA:RNA) and 0.32 Å (LNA1:RNA) for the entire ensemble of 40 structures. By inspection of the DNA:RNA ensemble, it is obvious that for the structures generated from B-form starting geometries some of the terminal nucleobases do not converge to a geometry identical with that of the structures generated from A-form starting geometry. As a consequence, we only include the 20 structures calculated from the A-form starting geometry (lowest force field energies) in further analyses for each hybrid.

The final hybrid average structures feature fairly low distance restraint energies (see Table 1) and low distance violations compared with the starting structures, and the RMSDs of the coupling constants (J_{RMSD}) for the NMR structures are lower than those for either starting structure (see Table 1). Furthermore, no violations larger than 0.45 Å were observed in any of the hybrid structures.

General Description of the Average Structures Calculated. A DNA:RNA hybrid possesses an overall topology intermediate of canonical A- and B-forms. In particular, the minor groove width is intermediate of that of DNA:DNA (B-form) duplexes and RNA:RNA (A-form) duplexes.[29−32] This global topology is a result of the inhomogeneous structure of the two hybrid strands, with the riboses featuring *N*-type sugar conformations and the deoxyriboses displaying frequent repuckering between *N*- and *S*-type conformations.[30,32,33] Thus, the DNA strand of DNA:RNA hybrids is conformationally flexible, while the RNA strand is rigid and A-like.

The calculated average structures are all within the domain of right-handed A-type helices as demonstrated by RMSD values of 1.7, 1.7, and 0.8 Å between DNA:RNA, LNA1:RNA, and LNA3:RNA, respectively, and the energy minimized A-form starting structures. In the three hybrids, all glycosidic angles correspond to anti conformations of the nucleobases, and Watson−Crick base pairing is maintained for all base pairs. The hybrids are relatively regular as shown by the nearly straight helix axes as calculated by CURVES 5.2,[34,35] thus showing that the LNA nucleotides can be incorporated into the nucleic acid framework without major disruptions. The LNA1:RNA hybrid is less regular than the two other hybrids. This is due to the ends of the duplex not adopting a regular A-form geometry. This is most likely an artifact of the structure determination, as we observe near identical chemical shifts for the residues in question in the DNA:RNA and the LNA1:RNA hybrids. In general, the sequential interproton distance restraints in the ends of the LNA1:RNA hybrid are longer than those in the DNA:RNA hybrid and this might impose the observed geometry. Views of the average structures determined for the three hybrids are presented in Figure 2.

Even though the overall duplex topology progressively changes toward A-form geometry upon inclusion of the modifications, some structural features prevail. In the ApT base pair steps, the thymine bases stack on the preceding adenine, while there is little/no intrastrand overlap between bases in the TpA:UpA steps. This lack of intrastrand stacking is alleviated by interstrand adenine−adenine stacking. Notably, we observe purine interstrand stacking between G3 and A17, A6 and A14, and G8 and A12 in each of the three hybrids. This interstrand stacking stabilizes the pyrimidine−purine base pair steps.

Helicoidal Parameters. A selection of helix parameters for the three hybrids is shown in Figure 3. X-displacement, Y-displacement, inclination, and tip are the helix parameters with which the global helix axes are determined.[34,35] Consequently, these parameters allow a direct comparison between different duplex forms and the structures determined. X-displacement and inclination are parameters discriminative of A- and B-form duplexes. We observe that each of the hybrids have values for X-displacement intermediate of typical A- and B-form values, with each hybrid showing little variation along the duplex. The LNA3:RNA hybrid is closer to A-form values than are the LNA1:RNA and DNA:RNA hybrids. LNA3:RNA and DNA:RNA display inclination values near A-form values while, singularly, LNA1:RNA has values close to that of B-form. This may be a consequence of the ends of this duplex

(28) Mooren, M. M.; Wijmenga, S. S.; Van der Marel, G. A.; Van Boom, J. H.; Hilbers, C. W. *Nucleic Acids Res.* **1994**, *22*, 2658.
(29) Fedoroff, O. Y.; Salazar, M.; Reid, B. R. *J. Mol. Biol.* **1993**, *233*, 509.
(30) Gonzáles, C.; Stec, W.; Reynolds, M.; James, T. L. *Biochemistry* **1995**, *34*, 4969.
(31) Bachelin, M.; Hessler, G.; Kurz, G.; Hacia, J. G.; Dervan, P. B.; Kessler, H. *Nature Struct. Biol.* **1998**, *5*, 271.
(32) Gyi, J. I.; Lane, A. N.; Conn, G. L.; Brown, T. *Biochemistry* **1998**, *37*, 73.
(33) Cheatham, T. E., III; Kollman, P. A. *J. Am. Chem. Soc.* **1997**, *119*, 4805.
(34) Lavery, R.; Sklenar, H. *J. Biomol. Struct. Dyn.* **1988**, *6*, 63.
(35) Lavery, R.; Sklenar, H. *J. Biomol. Struct. Dyn.* **1989**, *7*, 655.

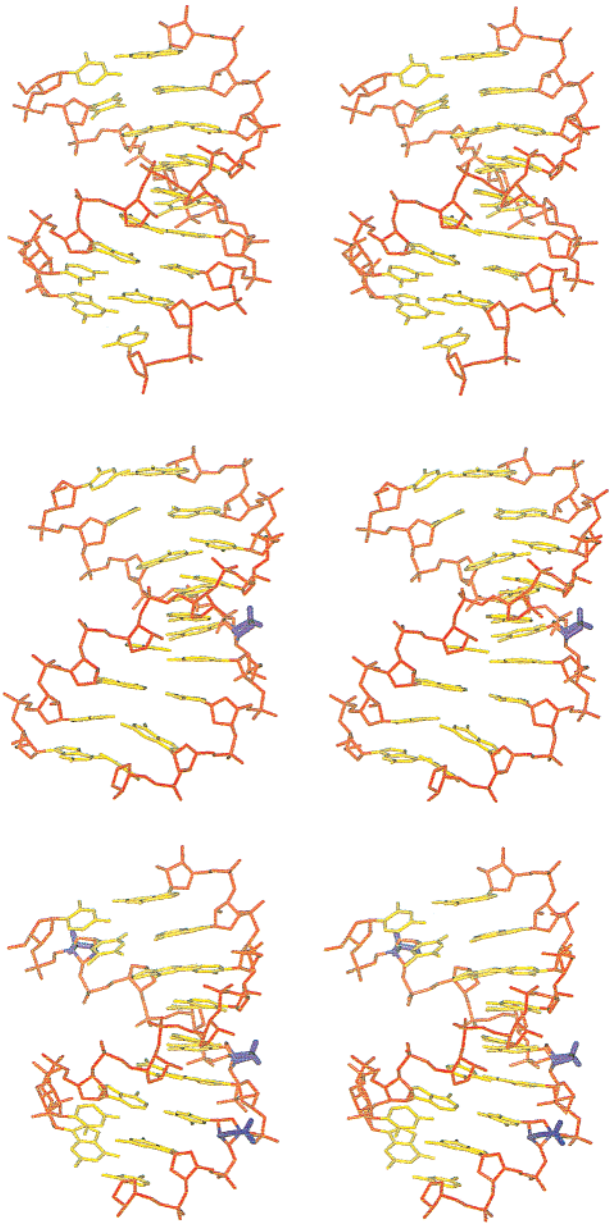

Figure 2. Stereoviews of the average structures of the three hybrids: DNA:RNA (top), LNA1:RNA (middle), and LNA3:RNA duplex (bottom). For clarity, only hydrogens on the modifications are shown. The coloring scheme is the following: the nucleobases, yellow; the sugar−phosphate backbone, red; and the LNA 2′-*O*,4′-*C* bridge, blue.

adopting irregular conformations as noted above. Y-displacement and tip, offering no discrimination of A- and B-form duplexes, merely serve to describe the regularity of the duplexes. We observe some changes along the duplexes (up to ∼1.0 Å for Y-displacement and up to ∼8° for tip), these changes seem to correlate between the hybrids and therefore might be sequence dependent.

The base-axis parameters are determined relative to the global helix axis and slight variation of the helix axes between the hybrids can influence the helicoidal parameters, thus rendering direct comparison of parameters between different duplexes troublesome. Forcing linear helix axes did not change the parameters significantly, and consequently we report the parameters determined with respect to nonlinear helix axes. Rise is near A-form values for the DNA:RNA and LNA3:RNA hybrids, while the LNA1:RNA hybrid displays some values closer to that of B-form. This is a mirror of the inclination parameter. Twist is a helix parameter poorly defined by NMR data,[36] and we observe variations along each of the duplexes. However, none of these variations can be attributed to the LNA modifications. Propeller twist is generally negative. The values are rather large compared with canonical A- and B-form values but large values for propeller twist appear to be common for NMR-derived structures.[37]

Sugar Conformations. The sugar puckers of the hybrids are listed in Table 2. In the unmodified hybrid, the deoxyriboses adopt sugar conformations between P = 71° (A4) and 174° (G3). For all deoxyribose residues, bar G3, the sugar puckers determined correspond to values between *N*- and *S*-type conformations. This is in accordance with other NMR structures of DNA:RNA hybrids.[30−32,38] In the LNA1:RNA hybrid, an identical picture is drawn with the deoxyriboses having pseudorotation angle values intermediate of *N*- and *S*-type stretching toward the *S*-range, except for $T^{L}5$ and A6, i.e. the LNA modified nucleotide and its 3′-flanker. These two nucleotides have *N*-type sugar puckers, with $P = 16°$ and 15°, respectively. A4, the 5′-LNA flanker, has a pseudorotation value of $P = 110°$ in accordance with the observation that this sugar is repuckering between *N*- and *S*-type conformations as inferred by inspection of DQF-COSY cross-peaks.[16] In the LNA3:RNA hybrid, all deoxyriboses adopt *N*-type conformations with pseudorotation angles between −9° and 36°. In all hybrids, the riboses in the RNA strands adopt *N*-type conformations with the pseudorotation angle ranging from −11° to 43°.[39]

Backbone Angles. As for backbone angles, most reside in the normal ranges for right-handed duplex structures. In the DNA:RNA hybrid, we observe a single instance where the α and γ angles are not in a predominant (g−, g+)-conformation, A4 (α, γ: g+, t), and in the LNA1:RNA hybrid one as well, A14 (α, γ: t, t). These inhomogeneities of the α and γ angles reflect the inherent dynamical nature of the sugar phosphate backbone and the fact that no backbone angle restraints were included in the simulated annealing protocol (except for the terminal residues in LNA1:RNA).

The β-angles are found exclusively in trans conformations in all hybrids. The ϵ and ζ angles in the hybrids are predominantly in B_I (ϵ, ζ: t, g−) conformations.

The δ and χ angles are correlated with the sugar pucker. The LNA and ribose nucleotides display narrow distributions of the δ angles near 60°, while the deoxyriboses, as a consequence of the intermediate sugar conformations, have distributions in the

(36) Konerding, D. E.; Cheatham, T. E., III; Kollman, P. A.; James, T. L. *J. Biomol. NMR.* **1999**, *13*, 119.
(37) Gotfredsen, C. H.; Spielmann, H. P.; Wengel, J.; Jacobsen, J. P. *Bioconj. Chem.* **1996**, *7*, 680.
(38) Fedoroff, O. Y.; Ge, Y.; Reid, B. R. *J. Mol. Biol.* **1997**, *269*, 225.
(39) In the average structure families calculated, we observe a very narrow distribution of sugar puckers for each nucleotide. This narrow envelope of sugar puckers, obviously, is not representative of the sugar conformation in cases where repuckering occurs but rather is a trapping of the sugar in what corresponds to an average structure. This is reflected in the error between the calculated and the experimental coupling constants (J_{RMSD} = 2.0 Hz for DNA:RNA and 2.5 Hz for LNA1:RNA). A more realistic ensemble of sugar conformations is generated by an rMD-tar procedure as shown by the lower J_{RMSD} value for these ensembles (1.4 Hz for DNA:RNA and 1.8 Hz for LNA1:RNA) due to repuckering between *N*- and *S*-type sugar conformations. However, overall the rMD-tar ensembles possess structural features akin to the average structures, and consequently we are discussing these structures. These results go to show that identical overall structures can be obtained with either the sugars trapped in intermediate conformations (∼O4′-*endo*) or with repuckering occurring. Further details of the rMD-tar calculations can be found in the Supporting Information.

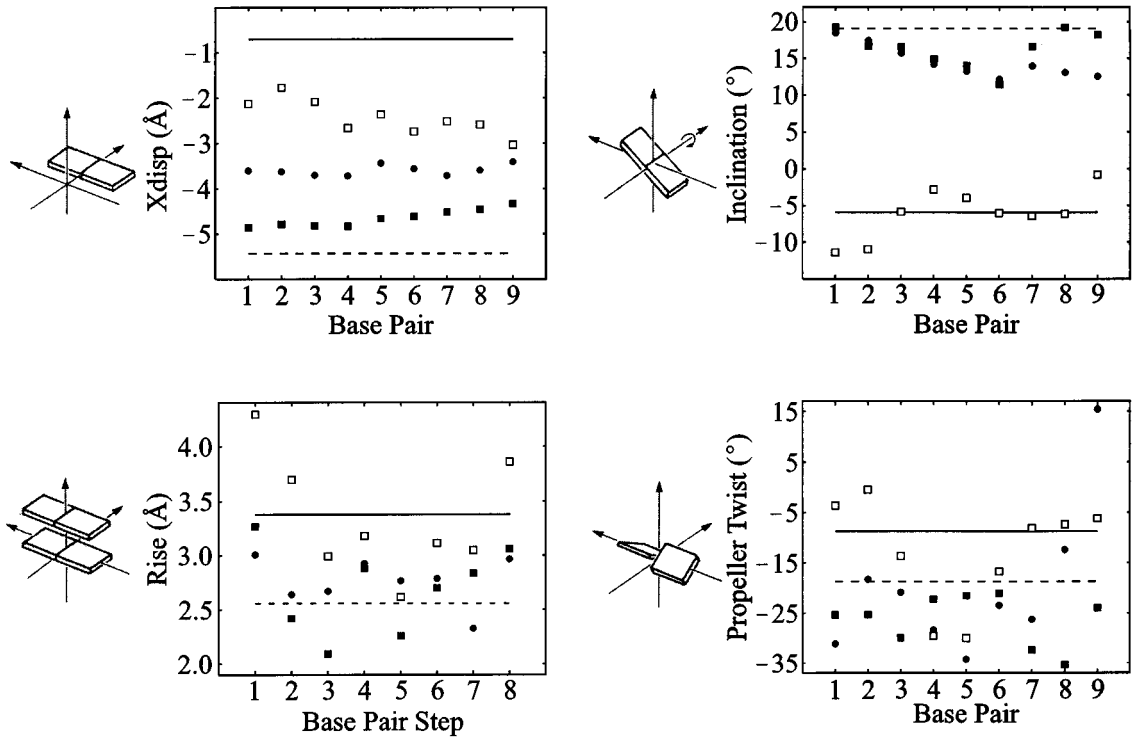

Figure 3. A few of the helicoidal parameters calculated for the three hybrids: DNA:RNA (●), LNA1:RNA (□), and LNA3:RNA (■). The parameters were calculated using CURVES 5.2 and are compared to those of canonical A-type duplex (---) and B-type duplex (—). For clarity, standard deviations are not shown.

Table 2. The Sugar Conformations of the DNA, LNA, and RNA Strands of the Various Hybrids Given by the Average Pseudorotation Angle (deg)[a]

	DNA:RNA	LNA1:RNA	LNA3:RNA
C1	73(3)	168(1)	−9(16)
T^L2/T2	132(2)	129(3)	17(1)
G3	174(1)	130(2)	8(1)
A4	71(3)	110(1)	36(4)
T^L5/T5	132(1)	16(0)	12(0)
A6	104(1)	15(7)	30(3)
T^L7/T7	144(7)	113(2)	16(0)
G8	95(1)	165(1)	3(1)
C9	86(1)	53(1)	18(1)
RNA-strand	−11 to 18	−11 to 43	1 to 29

[a] Standard deviations from the family of structures calculated are given in brackets.

Table 3. Minor Groove Widths for the Structures of the Various Hybrids as Represented by Average Interstrand Phosphorus Distances (Å)[a]

	DNA:RNA	LNA1:RNA	LNA3:RNA
P_4—P_{18}	14.7(0.2)	14.8(0.1)	15.6(0.2)
P_5—P_{17}	15.5(0.2)	15.4(0.1)	15.8(0.2)
P_6—P_{16}	13.6(0.2)	15.0(0.2)	15.7(0.1)
P_7—P_{15}	13.4(0.1)	14.8(0.1)	15.3(0.1)
P_8—P_{14}	13.7(0.4)	14.5(0.1)	15.1(0.1)
P_9—P_{13}	16.3(0.1)	13.6(0.2)	15.0(0.1)
average	14.5	14.7	15.4

[a] Standard deviations from the family of structures calculated are given in brackets.

range from 70° to 150°. The glycosidic angles have slightly lower values for LNA and ribose nucleotides (ca. −160°) than for deoxyriboses (ca. −130°).

Proton phosphorus coupling constants can yield experimental evidence for backbone conformations. From *J*-scaled ^{1}H−^{31}P HMBC spectra, we were able to gauge values for $^3J_{H3'P}$, $^4J_{H4'P}$, and $^4J_{H2'P}$. However, a quantitative determination of most of these coupling constants was precluded due to severe spectral overlap. Generally, we find $^3J_{H3'P} \simeq 6-8$ Hz for ribo- and LNA-nucleotides and $^3J_{H3'P} \simeq 2-4.5$ Hz for deoxyriboses, these coupling constants being consistent with ϵ angles in the trans range and with slightly larger ϵ angles for ribo- and LNA-nucleotides than for deoxyribonucleotides.[28] Vanishing $^4J_{H2'P}$ coupling constants corroborate the trans conformation for ϵ.[40] By and large we observe nonvanishing $^4J_{H4'P}$ coupling constants, i.e. with values of 1−2 Hz. A rigorous determination of the coupling constants is impossible but nonvanishing values are only possible with a (β, γ: t, g+) conformation as found in the hybrid structures determined.[40]

Summarizing, the backbone angles generally fall in the ranges expected for nucleic acids in all of the hybrids, i.e. we cannot determine any conspicuous changes in the backbone conformation attributable to the LNA modifications.

Minor Groove Width. The minor groove width depends on the overall duplex conformation, B-type duplexes having a minor groove width of ∼11.5 Å and A-type duplexes having a much wider minor groove of ∼16.8 Å, with the minor groove width taken as the shortest interstrand phosphorus distance. In our structures, the minor groove is progressively widened upon introduction of LNA modifications (Table 3). Thus the average minor groove width is largest in the LNA3:RNA hybrid and smallest in the unmodified DNA:RNA hybrid. In the unmodified duplex, we observe a narrowing from the center toward the DNA 3′-end of the duplex. In the modified duplexes, however, a more uniform minor groove width is observed within each hybrid. Hence it seems the introduction of modifications "quenches"

(40) Wijmenga, S. S.; van Buuren, B. N. M. *Prog. Nucl. Magn. Reson. Spectrosc.* **1998**, *32*, 287.

this narrowing of the minor groove. Altogether, the minor groove widths of the DNA:RNA and LNA1:RNA hybrids are intermediate between A- and B-form structures, while the LNA3:RNA hybrid possesses a minor groove only slightly narrower than that of a canonical A-form duplex.

Discussion

Summary of Structural Features. In agreement with our previously published CD and NMR data,[16] the hybrids adopt overall A-like duplex structures, with the LNA nucleotides positioned as to partake in base stacking and Watson−Crick base pairing. We observe no significant changes in backbone angles in any of the hybrids compared with unmodified DNA or RNA. This demonstrates that LNA nucleotides can fit into the Watson−Crick nucleic acid duplex framework without any rearrangement of the backbone necessary. Moreover, our structures reproduce the sugar puckers determined by pseudorotational analysis of coupling constants quite well. That is, all ribonucleotides, including the LNA nucleotides, are in a pure *N*-type conformation, while we observe dramatic changes in the sugar puckering of the deoxyriboses of the hybrids upon introduction of either one or three modifications. In the DNA:RNA hybrid, all deoxyriboses are in conformations between *N*- and *S*-type, while in the LNA1:RNA hybrid, A6, the 3′-flanking nucleotide of the single LNA modification is in an *N*-type conformation. In the LNA3:RNA hybrid, the situation in the deoxyribose strand is perturbed dramatically with all sugars adopting *N*-type conformations. As a result of the alterations in the sugar conformations, the overall duplex conformation changes progressively toward A-type with an increasing number of LNA modifications. This is mirrored in a broadening of the minor groove and a shortening of intrastrand phosphorus distances.

Taken overall, it appears that with the inclusion of three LNA nucleotides, the number of LNA modifications has reached a saturation level with respect to structural changes and that further incorporations would furnish only minute changes in the duplex structure. This correlates well with the observation that the relative increase in helical thermostability per LNA nucleotide, relative to native reference duplexes, reaches a maximum for mix-mer LNAs containing less than 50% LNA nucleotides.[7,9]

RNase H Activity of LNA:RNA Hybrids. In the context of antisense activity, the adoption of an A-like structure, as observed for the LNA3:RNA hybrid, would presumably lead to inactivation of RNase H, as it is believed that a minor groove width intermediate of A- and B-type duplexes, i.e. that of a DNA:RNA hybrid, is the key determinant in RNase H recognition and subsequent scission of the RNA strand.[29,41] Indeed, in recent in vitro *E. coli* RNase H assays of LNA:RNA hybrids, it is observed that these hybrids are unable to elicit RNase H activity.[42] However, successful activation of RNase H by mix-mer LNA:RNA hybrids has been reported previously.[11] Thus it appears that further probing of the RNase H activity of LNA:RNA hybrids is necessary to fully understand the interplay between LNA nucleotide modifications, hybrid conformation, and RNase H activity.

The Conformational Changes Induced by LNA Modifications. Both NOE data and *J* coupling constants show that in the LNA1:RNA hybrid, the sugar conformation of A6 is changed to an *N*-type conformation while the sugar of A4 is unperturbed relative to the unmodified hybrid. How this discretion of directional conformational steering is achieved is intriguing, and below we shall attempt to rationalize this property by discussing possible explanations.

(i) A restriction of the sugar−phosphate backbone angles due to the locked sugar of LNA is a possibility. However, our structure and the rMD-tar calculation of the LNA1:RNA hybrid and unrestrained MD calculations of a fully modified LNA:RNA hybrid give no hint whatsoever of this. Additionally, we have seen above that the backbone angles of the LNA3:RNA hybrid are very similar to unmodified DNA and RNA duplexes. Finally, an LNA stereoisomer, α-L-LNA, does not perturb the sugar conformations of neighboring nucleotides when incorporated into DNA:RNA hybrids.[43] Hence this explanation appears unlikely.

(ii) The 2′-*O*,4′-*C*-methylene bridge is positioned in the minor groove pointing toward the 3′-neighboring nucleotide. To avoid steric clashes, the 3′-neighboring nucleotide might shift its sugar conformation toward an *N*-type conformation. Unrestrained MD calculations, though, show that an LNA-containing sequence can accommodate both *N*- and *S*-type nucleotides in the 3′-direction.

(iii) The A-type geometry of the LNA nucleotides imposes an A-type geometry of the 3′-flanking nucleotide to maximize stacking between the nucleobases. In the LNA:RNA hybrids we do not observe any stacking overlap between the LNA thymines and the 3′-flanking guanines or adenines. These nucleobases rather stack with purines of the base paired RNA strand. In addition, an identical gross stacking pattern is observed in the unmodified hybrid and, as such, a change in sugar conformation of the LNA 3′-flankers does not appear to be a prerequisite to obtain the favorable interstrand stacking in pyrimidine−purine base steps. Similarly, in an LNA:DNA hybrid with a T^{L}pA:TpA base step,[18] the 3′ flanking adenosine sugar possesses ∼40% *N*-type conformation, yet no intrastrand T^{L}-A or interstrand A-A overlap is occurring.

(iv) A fourth possibility is formation of a water-mediated hydrogen bond between an LNA nucleotide and the following deoxyribose (O2′(*n*) to O4′(*n*+1)), thus stabilizing an *N*-type conformation of this sugar. Measurement shows a distance of ∼4 Å between T^{L}(*n*) O2′ and N(*n*+1) O4′ in the LNA3:RNA hybrid and hence that a water-mediated hydrogen bond is possible although no stable hydrogen network is observed during the rMD-tar calculation of neither this nor the LNA1:RNA hybrid.

(v) Another explanation might be the change in electronic density at the brim of the minor groove introduced by the modification altering the pseudorotational profile of the 3′-flanking nucleotide (Figure 4). This hypothesis cannot be validated by simple force field methods but rather requires high-level quantum mechanical calculations. However, we observe a distinct change (∼1 ppm) in ^{31}P chemical shift of the LNA phosphates. This shift, as not imposed by a change in backbone geometry, most likely is attributable to a change in electronic

(41) Toulmé,J.-J.; Tidd, D. In *Ribonucleases H*; Crouch, R. J., e.al., Eds.; INSERM: Paris, France, 1998; pp 225−250.
(42) Sørensen, M. D.; Kværnø, L.; Bryld, T.; Håkansson, A. E.; Verbeure, B.; Gaubert, G.; Herdewijn, P.; Wengel, J. *J. Am. Chem. Soc* **2002**, *124*, 2164−2176.
(43) Petersen, M.; Håkansson, A. E.; Wengel, J.; Jacobsen, J. P. *J. Am. Chem. Soc.* **2001**, *123*, 7431.

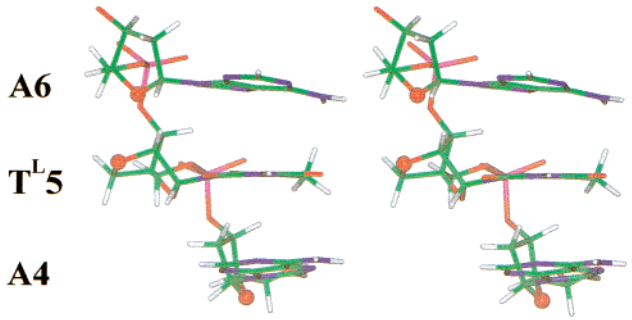

Figure 4. Stereoview close-up of the A4-T^{L}5-A6 fragment of the LNA3:RNA hybrid. O2′ of the LNA modification T^{L}5 and O4′ in A4 and A6 are shown as balls. The distances are T^{L}5:O2′−A6:O4′ = 3.7 Å and T^{L}5:O2′−A4:O4′ = 8.0 Å. The coloring scheme is the following: carbon, green; hydrogen, off-white; nitrogen, blue; oxygen, red; and phosphorus, magenta.

density in the minor groove wall as compared with unmodified nucleic acids.

This last explanation appears the most appealing since it complies with, and explains, all our experimental data. However, on the basis of the data presented, it is not possible to distinguish a water-mediated effect from an electrostatic interaction. A direct consequence of this hypothesis would be that the O2′ oxygen is the structural feature of LNA inducing the conformational change of the 3′-neighboring nucleotide.[44] Comparison with structural studies of duplexes containing nucleotides with an oxygen in the 2′-position flanked by deoxynucleotides would serve to validate this hypothesis.

Comparison with the Literature. There is only one study of an RNA/DNA:RNA hybrid in the literature, in which Szyperski et al.[45] have studied r(GCCA)d(CTGC):r(GCAGUGGC) finding $J_{H1'H2'} < 2$ Hz for the deoxyribose immediately following the RNA stretch in the 3′-direction. This indicates that this deoxyribose sugar has a pure *N*-type sugar conformation. The remaining deoxyriboses display $J_{H1'H2'}$ coupling constants in accordance with *N*/*S* sugar equilibria. Jaishree et al.[46] have studied two mixed RNA/DNA hybrids. In a hexamer [d(CG)r(CG)d(CG)]$_2$, they measured sugar coupling constants which yielded 100% *S*-type conformation for G2 and 40% *S*-type conformation for C5 when interpreted in *N*/*S*-type sugar equilibria. These examples show that when neighboring riboses, deoxyriboses are more easily perturbed in the 3′-direction. However, in an octamer studied by Jaishree et al., [d(CG)r(C)d(TAGCG)]$_2$, neither G2 nor T4 show any perturbation caused by the ribonucleotide between. Thus it seems a ribose:ribose base pair is a prerequisite for extensive conformational changes of neighboring deoxyriboses. This may be a consequence of a ribose:ribose base pair, in contrast to a deoxyribose:ribose base pair, adopting a conformation with the O2′ oxygen in a favorable position for interacting with the 3′-neighboring sugar.

In an interesting study, Nishizaki et al.[47] have studied a partly modified 2′-OMe DNA:RNA hybrid with the sequence d(G$_m$U$_m$C$_m$ATCTC$_m$C$_m$):r(GGAGAUGAC), where subscript m denotes a 2′-OMe-modified nucleotide. The RNA strand of this duplex is specifically cleaved by RNase H at the U15-G16 base step.[47] 2′-OMe-modified nucleotides adopt an *N*-type sugar conformation due to the electronegative 2′-oxygen atom[6] and overall the above modified hybrid adopts an A-type duplex conformation. The sugar conformations of the deoxyriboses were not extensively analyzed in terms of a two-state model; however, inspection of the DQF-COSY spectrum shown (Figure 1a in ref 47) indicates that A4, located 3′-flanking of a 2′-OMe modification, is in a pure *N*-type conformation (the H1′-H2′ cross-peak is canceled) while T5 and C6 may be in *N*/*S* equilibria. T7 has overlapping H1′-H2′ and H1′-H2″ cross-peaks, thus precluding any analysis. Altogether, a 2′-OMe nucleotide (adopting an *N*-type sugar conformation similar to that of LNA) seems to induce an effect similar to that of an LNA nucleotide.

From the above, it appears generally that in a (5′-ribose-deoxyribose-3′):(5′-ribose-ribose-3′) fragment, the deoxyribose sugar would be perturbed strongly toward an *N*-type conformation, and in a (5′-ribose-deoxyribose-3′):(5′-deoxyribose-ribose-3′) fragment, the deoxyribose positioned in the 3′-direction of the ribose is most susceptible to perturbation. The conformational changes induced by ribonucleotides are quite similar to those induced by LNA nucleotides, thereby supporting our hypothesis.

The Increased Stability of LNA:RNA Hybrids. Originally, LNA was designed as an RNA mimic preorganized for binding to RNA. Studies of ssLNA[19] and the present studies of LNA:RNA hybrids show that this indeed is the case. Both in the single stranded state and in the duplex state, the locked sugar moiety of LNA assumes an RNA-like (*N*-type) conformation while neighboring deoxyribonucleotides are perturbed toward an RNA-like conformation as well.

How these structural features translate into an increased thermostability is an intriguing structure−activity problem. It is widely demonstrated that nucleic acid modifications, which increase the *N*-like character of sugars in DNA strands, yield an increased thermostability of DNA:RNA hybrids.[6] Generally, this increased helical stability is attributed to a more efficient base stacking made possible by the modified hybrid adopting an A-form geometry.[23] The substantial increase in the helical stability of LNA:RNA hybrids may, at least partly, stem from the introduction of more A-like structures relative to the structure of DNA:RNA hybrids. However, by inspection of our structures, we observe no apparent gross change in stacking geometries. This is not to say that the stacking energies are unchanged upon introduction of LNA modifications as relatively minor changes in geometry may yield such changes. Quantification of base stacking energies would, however, require laborious high-level quantum mechanical calculations outside the scope of this work.

Another contribution stems from the locked sugar moiety of LNA. This decreases/removes the entropic gain occurring on denaturation of an LNA:RNA hybrid by making ssLNA less advantageous than free ssDNA. So introducing LNA modifications into the deoxyribose strands of DNA:RNA hybrids appears to entail an entropic advantage.[12]

(44) Thio-LNAs, i.e. LNAs with the 2′-oxygen replaced with a 2′-sulfur, display helical thermostabilities comparable to those of LNA [Kumar, R.; Singh, S. K.; Koshkin, A. A.; Rajwanshi, V. K.; Meldgaard, M.; Wengel, J. *Bioorg. Med. Chem. Lett.* **1998**, *8*, 2219]. If our hypothesis as presented is true, one may expect thio-LNAs, with the less electronegative sulfur atom at the 2′-position, to have structural implications differing from those of LNA. We are currently investigating this aspect.

(45) Szyperski, T.; Götte, M.; Billeter, M.; Perola, E.; Cellar, L.; Heumann, H.; Wüthrich, K. *J. Biomol. NMR.* **1999**, *13*, 343.

(46) Jaishree, T. N.; Van der Marel, G. A.; Van Boom, J. H.; Wang, A. H. J. *Biochemistry* **1993**, *32*, 4903.

(47) Nishizaki, T.; Iwai, S.; Ohtsuka, E.; Nakamura, H. *Biochemistry* **1997**, *36*, 2577.

A change in the charge distribution of the minor groove wall, as proposed, would most likely furnish changes in solvation near LNA nucleotides. Such effects are intrinsically difficult to study, but a more favorable solvation of LNA-modified hybrids can be a contributing factor to the stability of LNA:RNA hybrids.

We note that LNA modifications induce a more substantial increase in helical thermostability than 2′-OMe modifications ($\Delta T_m \sim 5$ °C vs ~1.5 °C per modification). Nonetheless, both LNA:RNA and 2′-OMeDNA:RNA hybrids adopt A-type duplex geometries.[48,49] Solvation effects are likely to be quite similar for both modifications.[50] As such, the key to the observed difference must lie in the single stranded states. One possible explanation would be that 2′-OMe modifications, in a single stranded state, intrinsically are more flexible than LNA, and therefore less prone to enter a duplex state.

Taken altogether, the entropy advantage from the locked sugar appears to be a major contribution to the helical stability of LNA:RNA hybrids, although enthalpy and solvation contributions cannot be ruled out.

Conclusion

We have determined high-resolution structures of two LNA:RNA hybrids along with the unmodified reference DNA:RNA hybrid. We find that the inclusion of the LNA modifications propels the duplex geometry toward A-type; however, this effect is not solely due to the geometry of the C3′-*endo* locked LNA nucleotides as these modified nucleotides steer the 3′-neighboring deoxyriboses into an *N*-type sugar geometry as well. We propose that this is due to the 2′-oxygen of LNA altering the charge distribution in the minor groove wall thus facilitating this conformational shift of its 3′-neighbor. The adaption of a more A-like geometry of LNA modified hybrids is probably a part of the explanation of the helical stability observed for these hybrids, though the single-stranded states as well as the solvation of the hybrids have to be considered when explaining LNA's increased helical stability properties.

Protein Data Bank Accession Codes. Coordinates and restraints employed in calculations have been deposited in the Protein Data Bank (accession codes: DNA:RNA, 1HG9; LNA1:RNA, 1HHW; LNA3:RNA, 1HHX).

Acknowledgment. We thank The Instrument Center for NMR Spectroscopy of Biological Macromolecules at The Carlsberg Laboratory, Copenhagen granted by The Danish Natural Science Research Council for providing spectrometer time at the 750 MHz spectrometer. Financial support from The Danish Natural Science Research Council and The Technical Research Council is acknowledged.

Supporting Information Available: Table giving RESP atomic charges and atom types for LNA thymine monomers and details of rMD and rMD-tar calculations of the three hybrids (PDF). This material is available free of charge via the Internet at http://pubs.acs.org.

JA012288D

(48) Popenda, M.; Biala, E.; Milecki, J.; Adamiak, R. W. *Nucleic Acids Res.* **1997**, *25*, 4589.
(49) Adamiak, D. A.; Milecki, J.; Popenda, M.; Adamiak, R. W.; Dauter, Z.; Rypniewski, W. R. *Nucleic Acids Res.* **1997**, *25*, 4599.
(50) Egli, M.; Minasov, G.; Teplova, M.; Kumar, R.; Wengel, J. *Chem. Commun.* **2001**, 651.